

UCLA



NP-315759: Optical probing of simultaneous Biermann battery and Weibel instability generated magnetic fields in over critical density plasma

26th Annual ATF Users' Meeting
March 26th-28th, 2024

Chan Joshi*, Chaojie Zhang*, Audrey Farrell†, Ken Marsh

*PIs, †Presenter

Funding Sources:

NSF Grant No. 2003354:003

DOE Grant No. DE-SC0010064

Proposal Overview

GRAND OBJECTIVES

- 1) Study self-organization phenomena in laboratory plasmas
- 2) Gain a qualitative understanding of seed fields that are amplified by the galactic dynamo in astrophysical scenarios
- 3) Produce and demonstrate a single platform that allows us to measure the Weibel instability and Biermann battery magnetic fields simultaneously

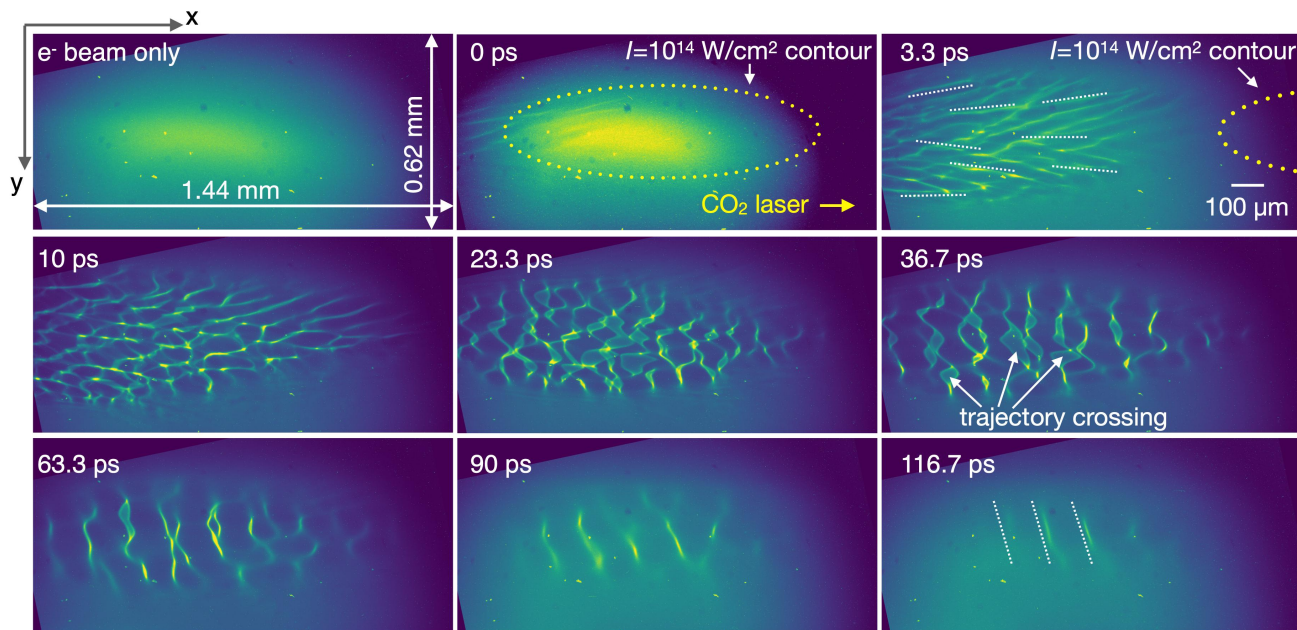
WHY ATF?

- 1) 2-5 TW class CO₂ laser to generate laser ionized plasmas over critical density
- 2) Synchronized 100fs, 800/400nm laser for Faraday rotation measurements
- 3) Potential extension to include collective Thomson scattering in the critical density region in the future

Self-Organization in Laboratory Plasmas

SELF-GENERATED MAGNETIC FIELDS

Evolution of the magnetic field k -spectrum is an example of self-organizing structures in tunnel ionized gases on a ps time scale.



First direct observation of the evolution of multi-dimensional Weibel instability. [C.J. Zhang et al. *PNAS* (2022), *RMPP* (2023)]

Where are self-generated fields important?

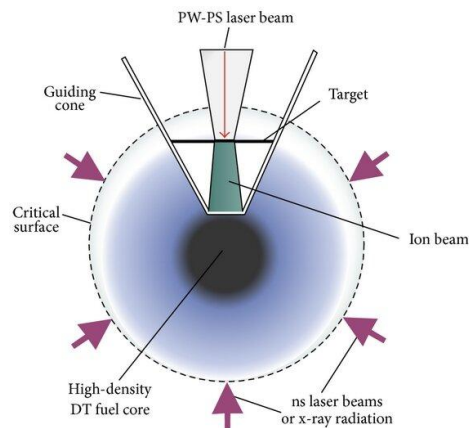
ASTROPHYSICS



Seed fields for galactic dynamo mechanism, γ -ray bursts

Figure reproduced from [Borlaff et al. *ApJ* (2023)]. See also: [Brandenburg & Ntormousi, *Annu. Rev. Astron. Astrophys.* (2023)]

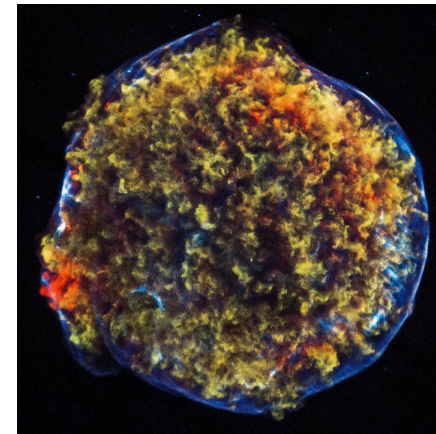
ENERGY



Laser-driven fusion schemes: fast ignition, indirect drive

Figure reproduced from [Ghoranneviss et al. *Sci. Technol. Nucl. Install.* (2014)]. See also: [Silva et al, *Phys. Plasmas* (2002)]

ACCELERATION



Collisionless shock acceleration

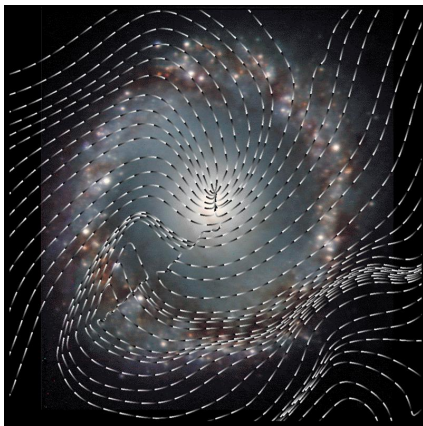
Image credit: NASA/CXC/SAO (2014)
See also: [Fiuza et al, *Phys. Rev. Lett.* (2012)], [Scharffer et al, *Phys. Rev. Lett.* (2017)]

Magnetogenesis in Space Plasmas

Growth of the magnetic fields we have observed in space plasmas, particularly in spiral galaxies such as our own, is most often attributed to the turbulent dynamo mechanism.

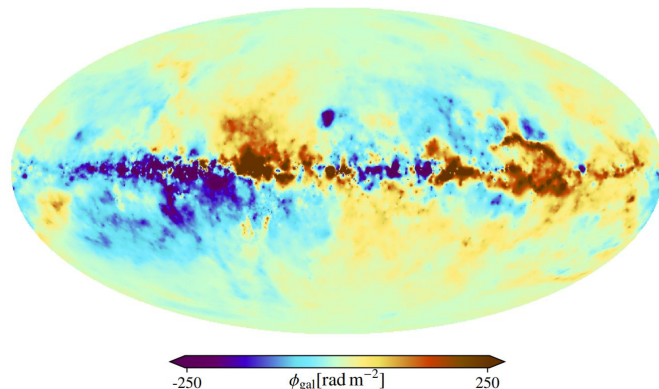
However, the dynamo requires a seed magnetic field to grow, the source of which is still debated.

Two major candidates for magnetogenesis are the Biermann battery and the Weibel instability.



Magnetic field streamlines in the center of the spiral galaxy NGC 1097. Figure from [Lopez-Rodriguez et al, *ApJ* (2021)]

[Kulsrud & Zweibel, *Rep. Prog. Phys.* (2008)]



Galactic Faraday rotation observed from Earth. Figure from [Huntschenreuter et al. *Astron. Astrophys.* (2021)]

The Biermann Battery

When nonparallel temperature and density gradients exist in a plasma, magnetic fields can be spontaneously generated through a mechanism known as the Biermann battery.

The Biermann battery is one of the few source terms in the magnetohydrodynamic (MHD) induction equation.

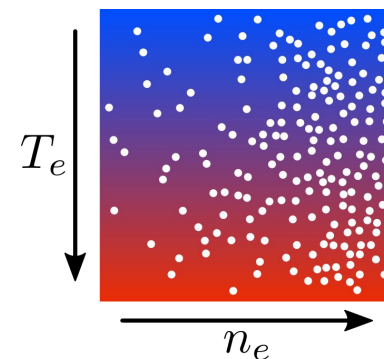
$$\frac{\partial \mathbf{B}}{\partial t} = \underbrace{\frac{\eta}{\mu_0} \nabla^2 \mathbf{B}}_{\text{diffusion}} + \underbrace{\nabla \times (\mathbf{v} \times \mathbf{B})}_{\text{advection}} - \underbrace{\nabla \times \frac{1}{en_e} (\mathbf{J} \times \mathbf{B})}_{\text{Hall effect}} + \underbrace{\frac{1}{en_e} \nabla T_e \times \nabla n_e}_{\text{Biermann battery}}$$

Biermann magnetic fields grow linearly at a rate inversely proportional to the density and temperature gradient scale lengths of the system.

$$B(t) \approx -\frac{t}{ce} \nabla n_e \times \nabla T_e \approx \frac{t}{ce} \frac{k_B T_e}{L_T L_n}$$

[Biermann, *Z. Naturforsch. Teil A* (1950)]

[Schoeffler et al, *Phys. Plasmas* (2014)]

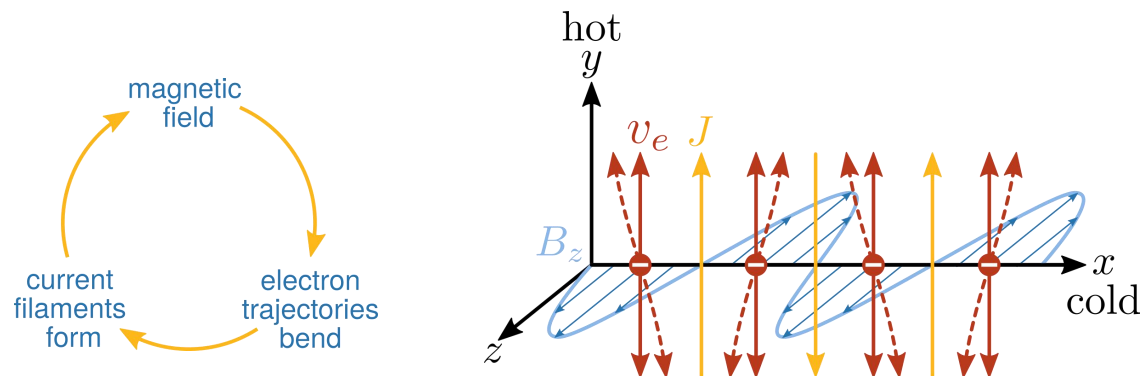


Perpendicular temperature (color) and density (particles) gradients resulting in a Biermann battery field out of the screen.

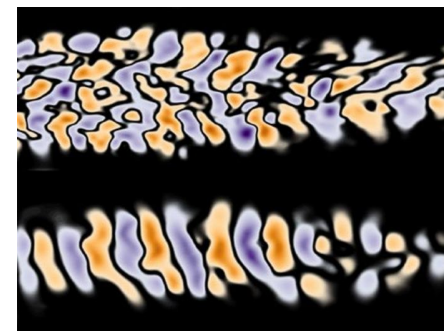
The Weibel Instability

The Weibel instability grows in the presence of anisotropic plasma temperatures, characterized by the anisotropy $A \equiv T_{\text{hot}}/T_{\text{cold}} - 1$ where T_{hot} and T_{cold} are temperatures in two orthogonal directions.

Weibel magnetic fields grow with an initially broad k -spectrum ($0 < k < A^{1/2} \omega_p / c$) in the cold direction, and coalesce to a quasi-single mode that can persist for many plasma periods.



[Weibel, *Phys. Rev. Lett.* (1959)]
 [Fried, *Phys. Fluids* (1959)]



Magnetic field contours showing self-organization due to Weibel

Coexistence of Biermann and Weibel Fields

BIERMANN BATTERY

- Macroscopic fields
- Driven by $\perp n_e$ and T_e gradients
- Fluid effect
- Grows linearly

WEIBEL INSTABILITY

- Microscopic fields
- Driven by anisotropic T_e
- Kinetic effect
- Grows exponentially

Both mechanisms have been characterized in separate experiments^{1,2}, but coexistence of the two in a single plasma has yet to be observed.

Can these two mechanisms coexist? Which mechanism dominates? Under what conditions?

The proposed experiment aims to characterize the evolution and interplay of simultaneous Biermann and Weibel magnetic fields for the first time.

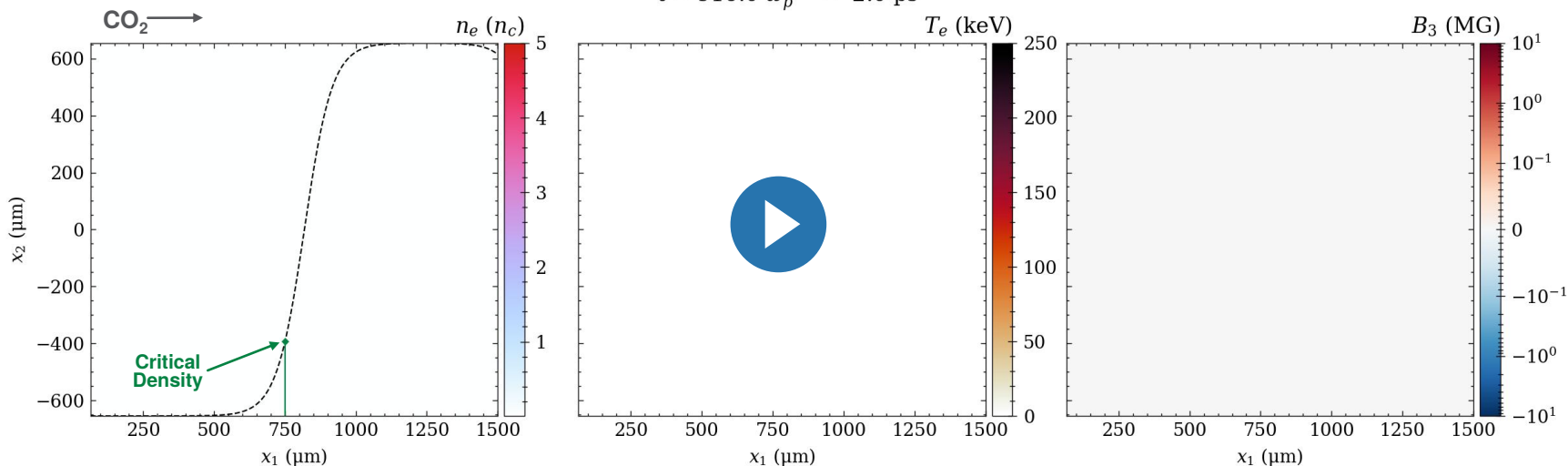
1. [Pilgram et al, *High Power Laser Sci. Eng.* (2022)]

2. [C.J. Zhang et al. *PNAS* (2022)]

2D3V PIC Simulations

We can show the interplay of Biermann and Weibel in self-consistent simulations using laser parameters consistent with ATF's CO₂ laser ($\lambda = 9.2\mu\text{m}$, LP in x_3 , $a_0 = 2.0$, 2.5 J, $w_0 = 35\mu\text{m}$ [$w_{\text{FWHM}} = 80\mu\text{m}$], $\tau_{\text{FWHM}} = 2\text{ps}$), incident on neutral hydrogen $n_0 = 5n_c = 6.6 \cdot 10^{19}\text{cm}^{-3}$ with a density ramp characterized by $L_n = 300d_e = 196\mu\text{m}$.

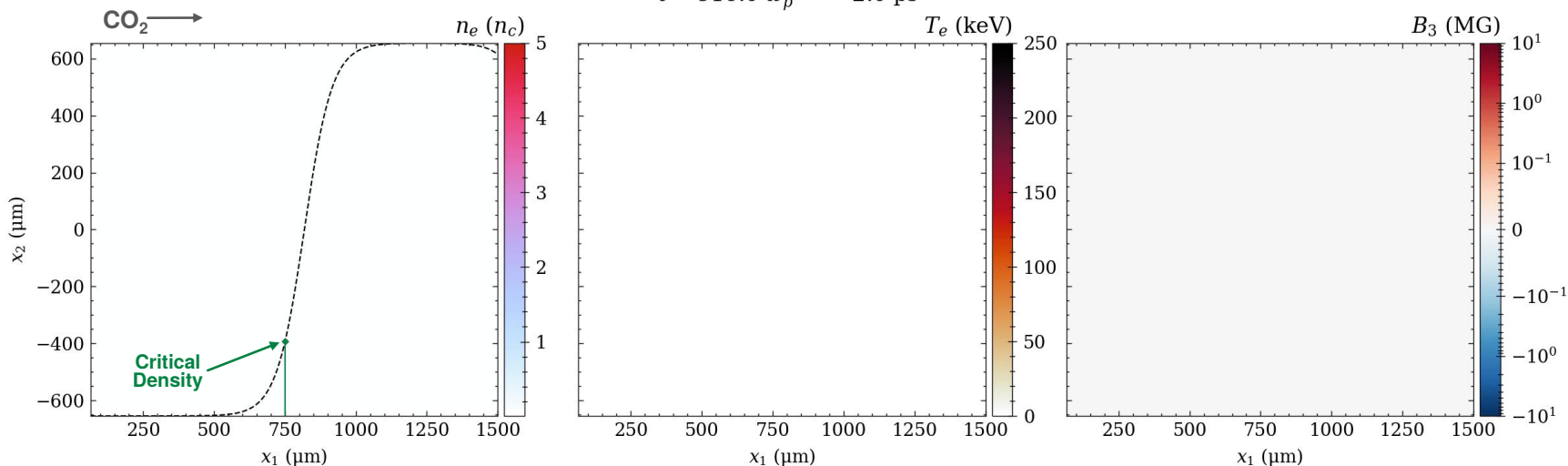
$$t = 916.0 \omega_p^{-1} = 2.0 \text{ ps}$$



2D3V PIC Simulations

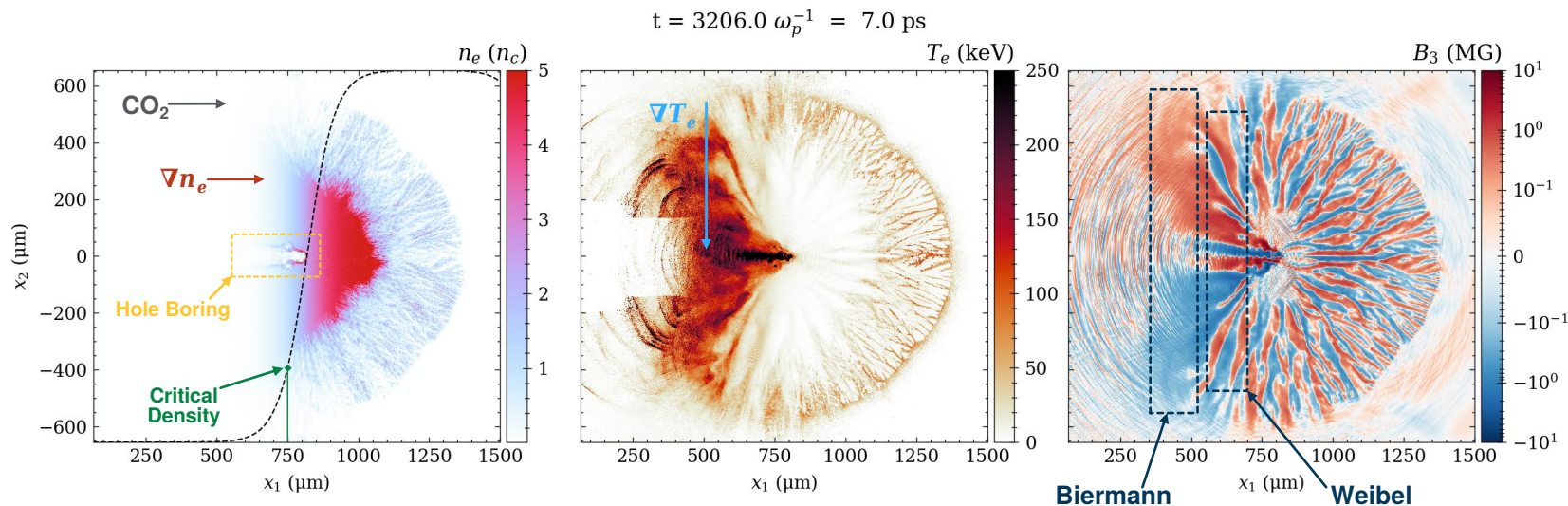
We can show the interplay of Biermann and Weibel in self-consistent simulations using laser parameters consistent with ATF's CO₂ laser ($\lambda = 9.2\mu\text{m}$, LP in x_3 , $a_0 = 2.0$, 2.5 J, $w_0 = 35\mu\text{m}$ [$w_{\text{FWHM}} = 80\mu\text{m}$], $\tau_{\text{FWHM}} = 2\text{ps}$), incident on neutral hydrogen $n_0 = 5n_c = 6.6 \cdot 10^{19}\text{cm}^{-3}$ with a density ramp characterized by $L_n = 300d_e = 196\mu\text{m}$.

$$t = 916.0 \omega_p^{-1} = 2.0 \text{ ps}$$



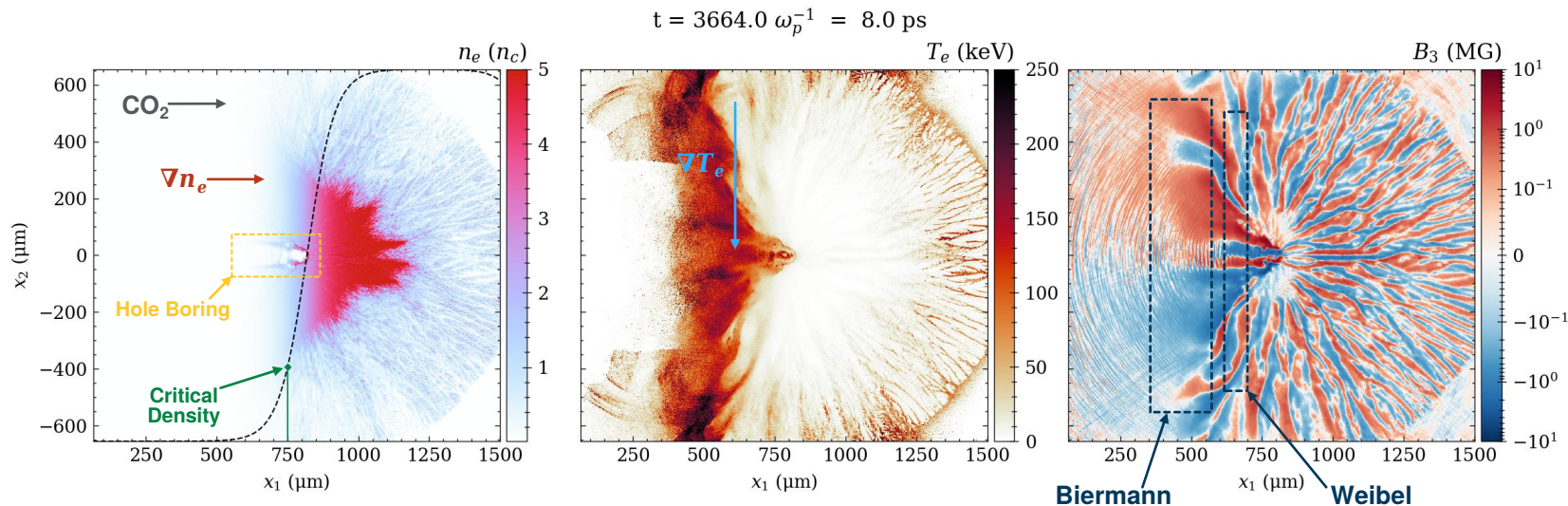
Simulated Magnetic Field Structures

Taking a closer look at a single time step, we can see Biermann structures in the azimuthal magnetic field transition to Weibel-like structures further into the target with field strengths exceeding 2MG. Beyond critical density the magnetic field is dominated by charge filaments.



Simulated Magnetic Field Structures

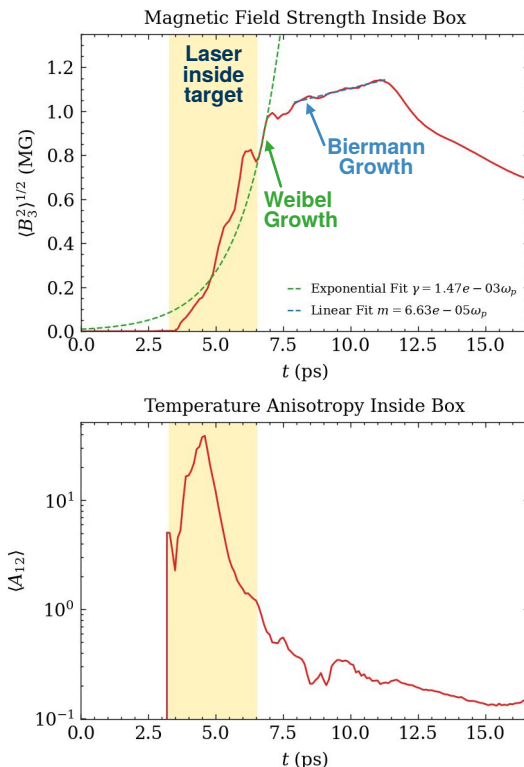
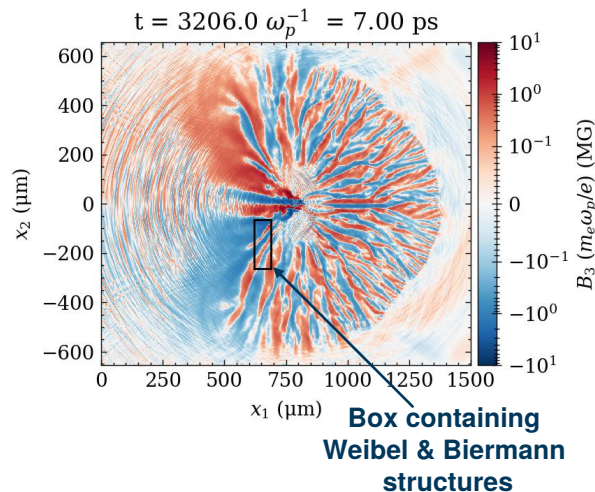
Taking a closer look at a single time step, we can see Biermann structures in the azimuthal magnetic field transition to Weibel-like structures further into the target with field strengths exceeding 2MG. Beyond critical density the magnetic field is dominated by charge filaments.



Simulated Magnetic Field Evolution

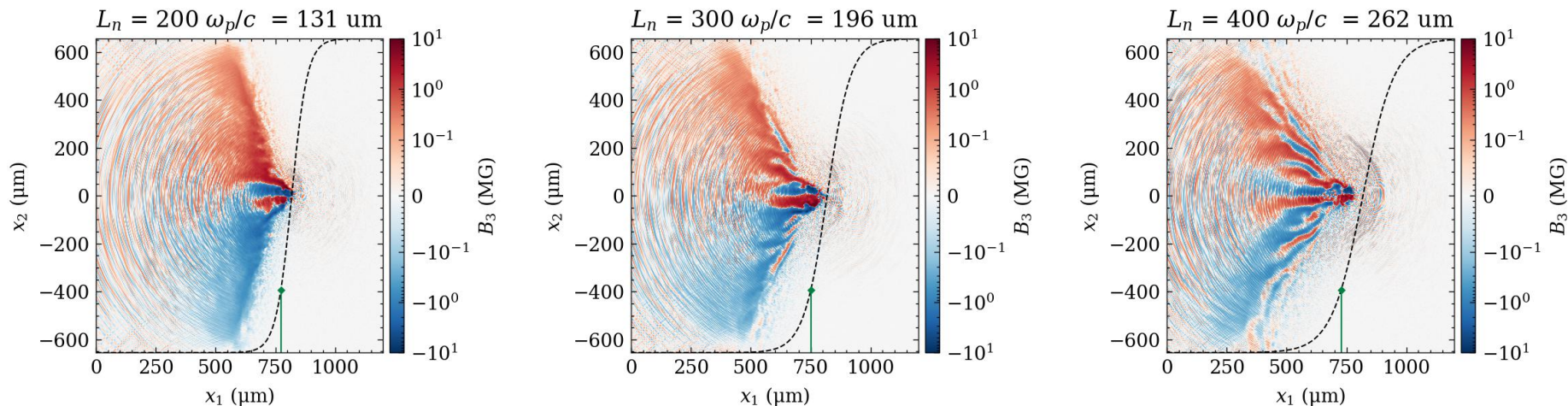
Selecting a small region in which both Weibel and Biermann structures develop in the simulation, we can compare the evolution of the magnetic field strength to theory for both mechanisms.

After the laser has left the target, we see a brief period of Weibel growth driven by the anisotropy between x_1 and x_2 , followed by a period of linear growth at a rate consistent with Biermann at the given density and temperature scale lengths.



Impact of Length Scale on Dominant Fields

By varying L_n and looking at the azimuthal magnetic fields after 7ps, we can see that at longer L_n Weibel fields dominate, while Biermann fields dominate at low L_n .



Biermann Dominated ←

→ Weibel Dominated

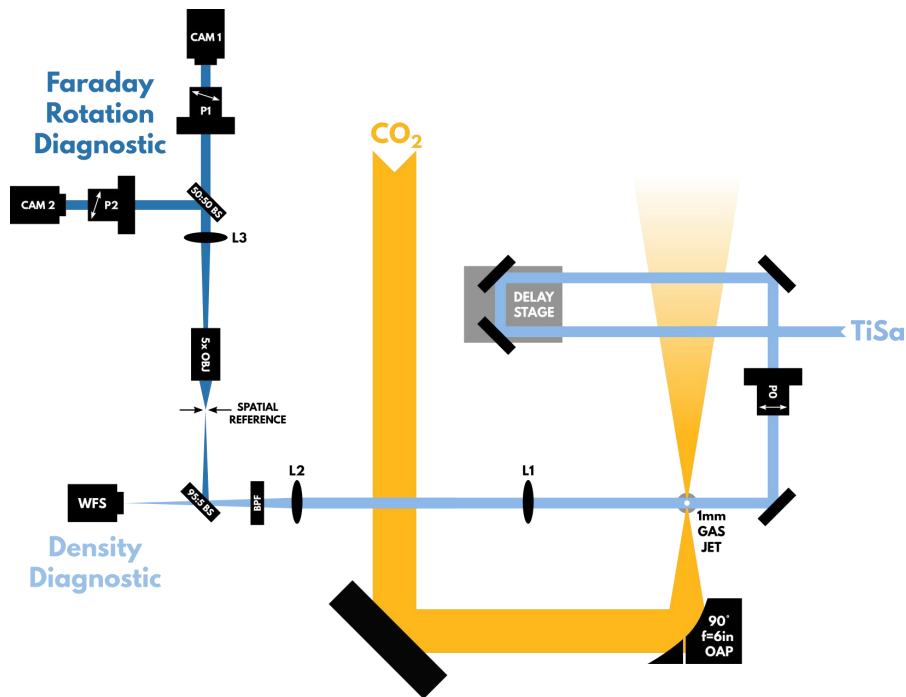
See also: [Shukla et al, *Phys. Rev. Research* (2020)]

Proposed Experiment

Since CO₂ critical density is transparent to Ti:Sapph, we plan to optically characterize the Biermann and Weibel magnetic fields using Faraday rotation. For the ~2MG magnetic fields seen in simulations, we expect 2-5deg rotation.

We have designed an imaging polarimeter using two cameras which can measure <1deg rotations in polarization with high spatial and temporal resolution. Coupled with a plasma density measurement, the polarization rotation measurement allows us to calculate magnetic fields along the probe propagation axis.

$$\phi_{\text{rot}} = \frac{e}{2m_e c n_c} \int_{\mathcal{P}} n_e \vec{B}_\varphi \cdot d\vec{\ell}$$

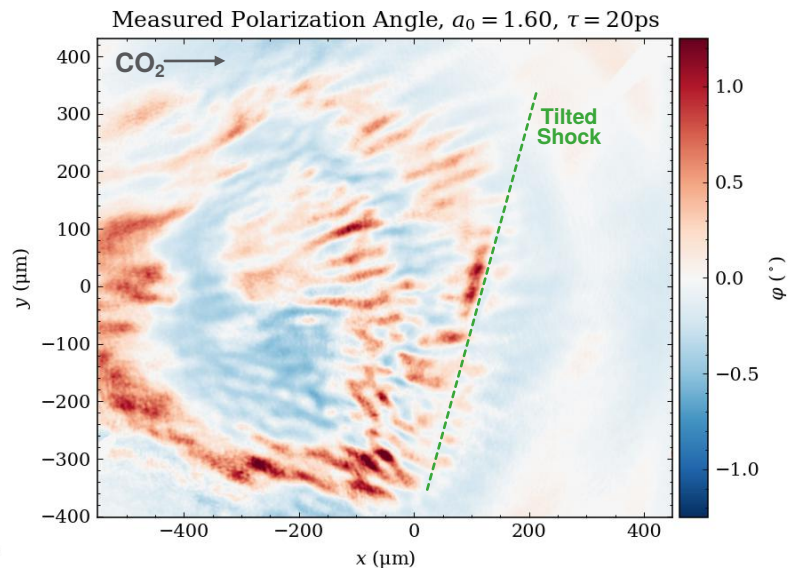
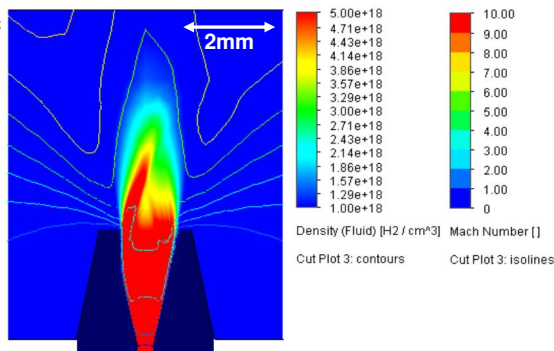


Preliminary Results from AE98 2023

During last year's experimental run of AE98, we had the opportunity to set up and test this diagnostic, recording the polarization rotation in near critical density plasmas in a density shock formed by an asymmetric gas jet nozzle.

While analysis of the measured Faraday rotation angles is still ongoing, preliminary results show clear structures in the polarization at angles $O(0.1 \text{ deg})$.

Flow simulation of the asymmetric gas jet nozzle showing the tilted density shock.



Experiment Requirements

CO₂ LASER

- 2-5J
- Single 2-3ps pulse
- Linear or circular polarization

TI:SAPPHIRE LASER

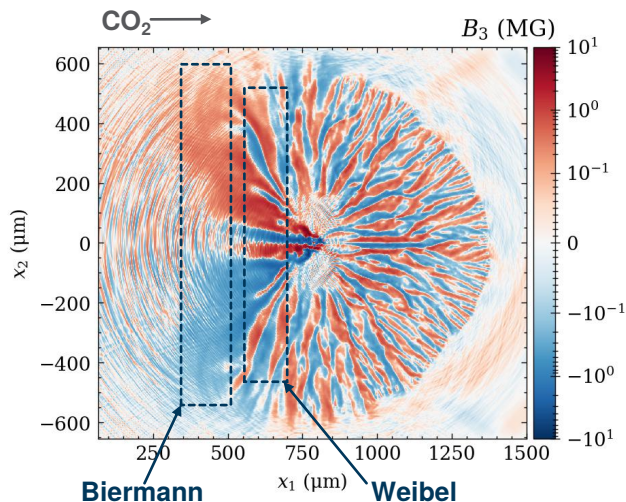
- 2-5 mJ
- Single 80fs pulse
- Linear polarization
- <0.2ps jitter relative to CO₂
- High pointing stability to maintain calibration of Faraday polarimeter

ADDITIONAL REQUIREMENTS

- Hydrogen and helium gas bottles
- 500-800psi backing pressures

Summary

Simulated azimuthal magnetic fields we aim to measure using Faraday rotation



- We propose a platform combining ATF's intense CO₂ laser and ultrashort Ti:Sapph laser to optically characterize self-generated magnetic fields
- Experiment Goals:
 - Observe for the first time the coexistence of Biermann battery and Weibel generated magnetic fields in a single plasma
 - Characterize the conditions in which either mechanism dominates the magnetic field
- We have demonstrated our diagnostics' capability in our previous work at ATF

Thank You

Electron Beam Requirements

Parameter	Units	Typical Values	Comments	Requested Values
Beam Energy	MeV	50-65	<i>Full range is ~15-75 MeV with highest beam quality at nominal values</i>	
Bunch Charge	nC	0.1-2.0	<i>Bunch length & emittance vary with charge</i>	
Compression	fs	Down to 100 fs (up to 1 kA peak current)	<i>A magnetic bunch compressor available to compress bunch down to ~100 fs. Beam quality is variable depending on charge and amount of compression required.</i> <i>NOTE: Further compression options are being developed to provide bunch lengths down to the ~10 fs level</i>	
Transverse size at IP (σ)	μm	30 – 100 (dependent on IP position)	<i>It is possible to achieve transverse sizes below 10 μm with special permanent magnet optics.</i>	
Normalized Emittance	μm	1 (at 0.3 nC)	<i>Variable with bunch charge</i>	
Rep. Rate (Hz)	Hz	1.5	<i>3 Hz also available if needed</i>	
Trains mode	---	Single bunch	<i>Multi-bunch mode available. Trains of 24 or 48 ns spaced bunches.</i>	

CO₂ Laser Requirements

Configuration	Parameter	Units	Typical Values	Comments	Requested Values
CO₂ Regenerative Amplifier Beam	Wavelength	μm	9.2	<i>Wavelength determined by mixed isotope gain media</i>	
	Peak Power	GW	~3		
	Pulse Mode	---	Single		
	Pulse Length	ps	2		
	Pulse Energy	mJ	6		
	M ²	---	~1.5		
	Repetition Rate	Hz	1.5	<i>3 Hz also available if needed</i>	
	Polarization	---	Linear	<i>Circular polarization available at slightly reduced power</i>	
	CO₂ CPA Beam	Wavelength	μm	9.2	<i>Wavelength determined by mixed isotope gain media</i>
Peak Power		TW	5	<i>~5 TW operation will become available shortly into this year's experimental run period. A 3-year development effort to achieve >10 TW and deliver to users is in progress.</i>	2-5
Pulse Mode		---	Single		Single
Pulse Length		ps	2		2
Pulse Energy		J	~5	<i>Maximum pulse energies of >10 J will become available within the next year</i>	2-5
M ²		---	~2		2
Repetition Rate		Hz	0.05		0.05
Polarization			Linear	<i>Adjustable linear polarization along with circular polarization can be provided upon request</i>	Linear & Circular

Other Experimental Laser Requirements

Ti:Sapphire Laser System	Units	Stage I Values	Stage II Values	Comments	Requested Values
Central Wavelength	nm	800	800	<i>Stage I parameters are presently available and setup to deliver Stage II parameters should be complete during FY22</i>	800
FWHM Bandwidth	nm	20	13		20
Compressed FWHM Pulse Width	fs	<50	<75	<i>Transport of compressed pulses will initially include a very limited number of experimental interaction points. Please consult with the ATF Team if you need this capability.</i>	75fs
Chirped FWHM Pulse Width	ps	50	50		
Chirped Energy	mJ	10	200		
Compressed Energy	mJ	7	~20	<i>20 mJ is presently operational with work underway this year to achieve our 100 mJ goal.</i>	5mJ
Energy to Experiments	mJ	>4.9	>80		
Power to Experiments	GW	>98	>1067		

Nd:YAG Laser System	Units	Typical Values	Comments	Requested Values
Wavelength	nm	1064	<i>Single pulse</i>	
Energy	mJ	5		
Pulse Width	ps	14		
Wavelength	nm	532	<i>Frequency doubled</i>	
Energy	mJ	0.5		
Pulse Width	ps	10		

Special Equipment Requirements and Hazards

- Electron Beam
 - N/A
- CO₂ Laser
 - Linear and circular polarization
- Ti:Sapphire and Nd:YAG Lasers
 - No special configurations needed.
- Hazards & Special Installation Requirements
 - Large installation (chamber, insertion device, etc.):
 - Cryogenics:
 - Introducing new magnetic elements:
 - Introducing new materials into the beam path:
 - Any other foreseeable beam line modifications:

Experimental Time Request

CY2024 Time Request

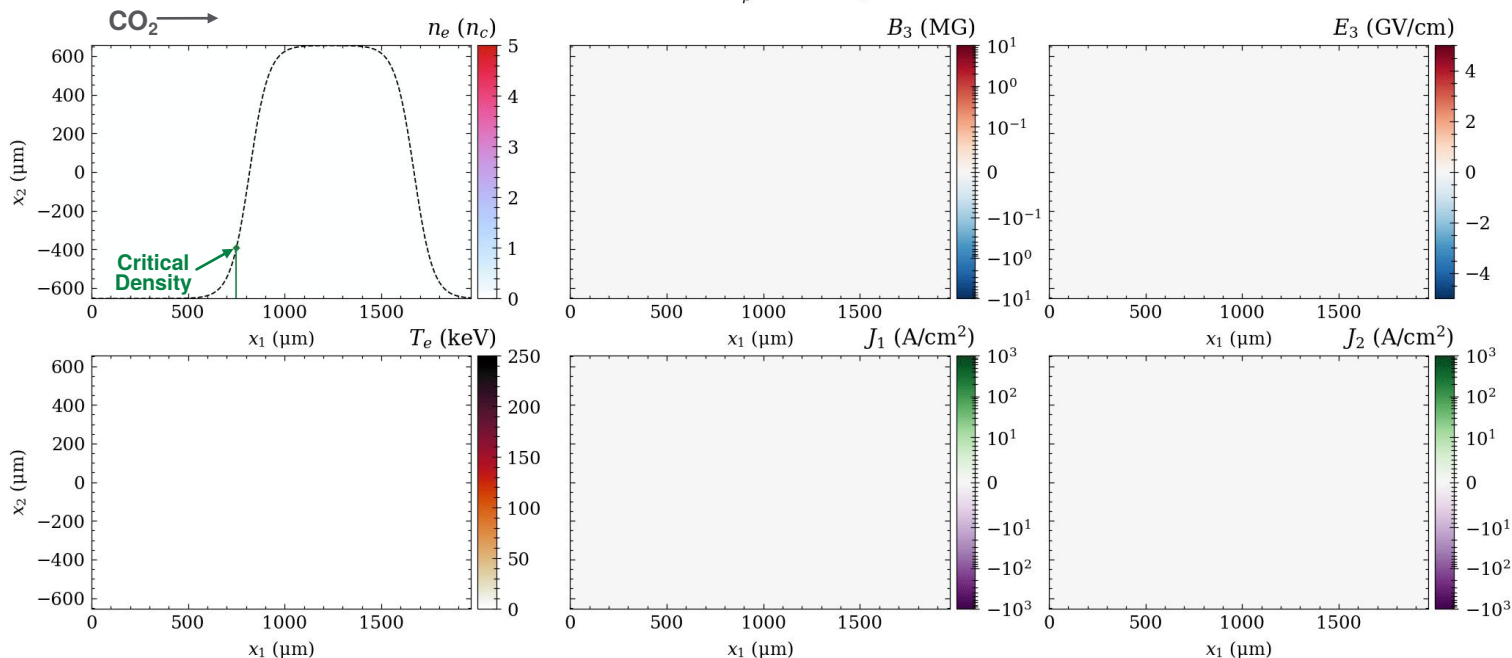
Capability	Setup Hours	Running Hours
Electron Beam		
NIR Laser	40	80
LWIR Laser	40	80

Total Time Request for the 3-year Experiment (including CY2024-26)

Capability	Setup Hours	Running Hours
Electron Beam		
NIR Laser	80	160
LWIR Laser	80	160

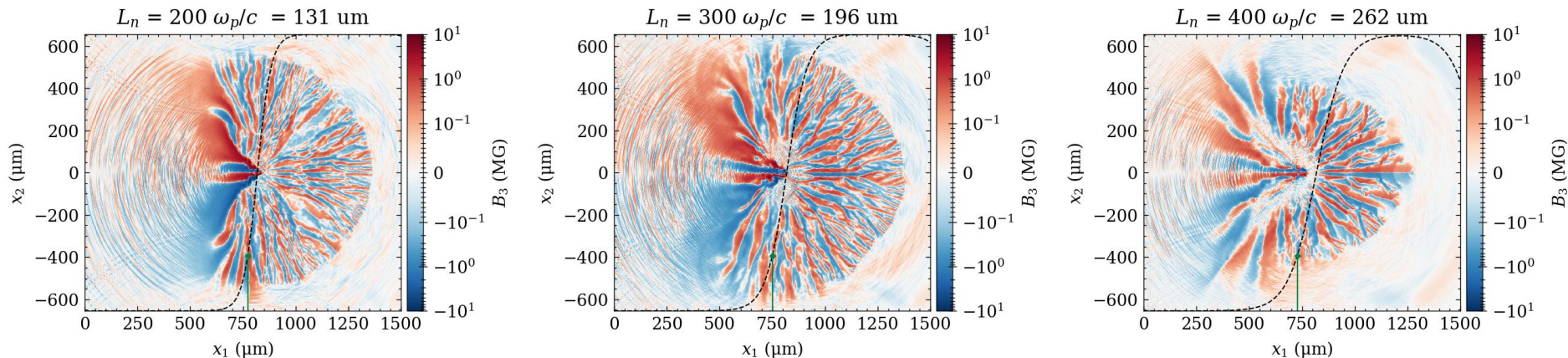
Backup: More Detailed Simulation Results

$\lambda = 9.2\mu\text{m}$, LP in x_3 , $a_0 = 2.0$ (2.5 J), $w_0 = 35\mu\text{m}$, $\tau_{\text{FWHM}} = 2\text{ps}$, $n_0 = 5n_c = 6.6 \cdot 10^{19}\text{cm}^{-3}$ H, $L_n = 300d_e = 196\mu\text{m}$
 $t = 0.0 \omega_p^{-1} = 0.00 \text{ ps}$



Backup: Length Scales in CO₂ Ionized Plasma

Varying L_n and looking at the azimuthal magnetic fields after 7ps. At longer L_n Weibel fields dominate, while Biermann fields dominate at low L_n .



See also: [Shukla et al, *Phys. Rev. Research* (2020)]

Backup: Detailed Faraday Analysis

Each of the cameras records two images, one before the plasma is formed and one after.

Intensity with no plasma:

$$I_{B\pm}(y, z) = s_{\pm}(y, z) I_B(y, z) \sin^2 \theta_{\text{pol}}$$

effective camera
sensitivity

probe beam
intensity

polarizer angle

intensity of unpolarized
plasma self-emission

Intensity with plasma:

$$I_{S\pm}(y, z) = s_{\pm}(y, z) \left[I_S(y, z) \sin^2(\varphi_{\text{rot}}(y, z) \pm \theta_{\text{pol}}) + \frac{I_{SE}(y, z)}{2} \right]$$

Taking the difference of the two normalized signals remove the self-emission effects:

$$\frac{I_{S+}}{I_{B+}} - \frac{I_{S-}}{I_{B-}} = \frac{I_S}{I_B} \frac{2 \sin(2\varphi_{\text{rot}})}{\tan \theta_{\text{pol}}}$$

$$\varphi_{\text{rot}}(y, z) = \frac{1}{2} \arcsin \left[\frac{I_B(y, z)}{I_S(y, z)} \left(\frac{I_{S+}(y, z)}{I_{B+}(y, z)} - \frac{I_{S-}(y, z)}{I_{B-}(y, z)} \right) \frac{\tan \theta_{\text{pol}}}{2} \right]$$

~1 for stable beams

[Swalding et al., *Rev Sci Instrum*, 2014]